2016 23rd International Conference on Pattern Recognition (ICPR)
Cancún Center, Cancún, México, December 4-8, 2016

Estimates of Classification Complexity for Myoelectric Pattern Recognition

Niclas Nilsson
Department of Signals and Systems
Chalmers University of Technology
Gothenburg, Sweden
Email: nniclas@student.chalmers.se

Max Ortiz-Catalan
Chalmers University of Technology
Gothenburg, Sweden
Sahlgrenska University Hospital
Gothenburg, Sweden
Integrum AB
Mölndal, Sweden
Email: maxo@chalmers.se

***Abstract*—Myoelectric pattern recognition (MPR) can be used for intuitive control of virtual and robotic effectors in clinical applications such as prosthetic limbs and the treatment of phantom limb pain. The conventional approach is to feed classifiers with descriptive electromyographic (EMG) features that represent the aimed movements. The complexity and consequently classification accuracy of MPR is highly affected by the separability of such features. In this study, classification complexity estimating algorithms were investigated as a potential tool to estimate MPR performance. An early prediction of MPR accuracy could inform the user of faulty data acquisition, as well as suggest the repetition or elimination of detrimental movements in the repository of classes. Two such algorithms, Nearest Neighbor Separability (NNS) and Separability Index (SI), were found to be highly correlated with classification accuracy in three commonly used classifiers for MPR (Linear Discriminant Analysis, Multi-Layer Perceptron, and Support Vector Machine). These Classification Complexity Estimating Algorithms (CCEAs) were implemented in the open source software BioPatRec and are available freely online. This work deepens the understanding of the complexity of MPR for the prediction of motor volition.**

I. Introduction

Myoelectric Pattern Recognition (MPR) has been shown to have great potential as part of the control strategy for a number of clinical applications, such as upper-limb prostheses control [1], phantom limb pain treatment [2] and rehabilitation after stroke [3]. Electromyography (EMG) is commonly acquired using surface electrodes (SEs) that are sensitive to changes in environmental conditions and motion artifacts [4], which makes frequent calibration or training of the applied pattern recognition algorithm (PRA) necessary. In order to acquire the data needed for such calibration or training, EMG is recorded while the patient performs muscle contractions relevant to the desired movements. Such recordings might be affected by errors due to the surface electrodes instability but also by human factors.

Reaz *et al.* suggested the analysis of important EMG attributes, such as the signal to noise ratio, in order to enable high MPR accuracy [5]. However, analyzing data based on these attributes requires experience and time. The literature on automated data analysis methods is limited despite the well-known consequences of using low quality recordings.

Apart from a few exceptions most studies on MPR use features that are extracted from raw EMG [6]. PRAs classification accuracy is highly dependent on the feature sets used as input, and therefore studies have been conducted on the performance of a variety of EMG features, as well as on the selection of such features [7], [8]. Liu *et al.* applied two feature selecting algorithms, Minimum Redundancy and Maximum Relevance (mRMR) and Markov Random Fields (MRF), to an electrode array setup [9]. The Kullback-Leibler Divergence was used in mRMR to rate relevance and redundancy of features and channels, which were ranked and selected into sets according to these ratings [10]. MRF was employed similarly to mRMR, but the features and channels were rated based on inter and intra class scatters, as well as total data scatter [11]. Bunderson *et al.* defined three data quality indices, namely Repeatability Index (RI), Mean Semi-principal Axis (MSA) and Separability Index (SI). These indices were used to rate the subjects ability to increase data quality when EMG was recorded repeatedly over several days [12]. Even though none of the studies above aimed to estimate classification complexity, they suggested useful ways to draw information from EMG when predicting classification accuracy.

Studies on Classification Complexity Estimates (CCEs) are more common outside the MPR field. Two nonparametric multiresolution complexity measures, Nearest Neighbor Separability (NNS) and Purity, were defined by Singh in 2003 [13]. These CCEs showed promising results but were not evaluated using EMG. Singh compared his results with a number of statistical similarity measures which were also potentially adequate CCEs. Among them were Kullback-Leibler Divergence, Bhattacharyya distance [14] and Mahalanobis distance [15]. In the present study these algorithms were used to describe the complexity of MPR to decode motor volition.

The aforementioned Classification Complexity Estimating Al-

978-1-5090-4847-2/16/$31.00 ©2016 IEEE

gorithms (CCEAs) were implemented in BioPatRec, which is an open source tool for the development and benchmarking of algorithms for advanced bioelectric control [16]. BioPatRec enables recording, preprocessing, feature extraction, pattern recognition and real-time control of artificial limbs using bioelectric signals. In the work presented here we evaluated the outcome of CCEAs and compared it with the accuracy of a number of classifiers. The resulted correlations provided evidence of CCEAs suitability to inform on MPR complexity. All code and data used in this study is available online [17].

II. Methods

A. Data Set

The data set used in this study is included in the BioPatRec data repository and is available online [17]. EMG was recorded in 20 subjects who performed 11 movements (Hand open/close, wrist flexion/extension, pro/supination, side grip, fine grip, agree or thumb up, pointer or index extension and rest) [16]. Disposable Ag/AgCl electrodes (⌀ = 1 cm) were place over the skin in bipolar configurations with 2 cm inter-electrode distance. The first channel was placed along the extensor carpi ulnaris mucle, and the rest (three) were equally spread around the most proximal third of the forearm. The more proximal electrode of every bi-pole was connected to the positive terminal of the amplifier.

B. Recording and Pre-Processing

The subjects were requested to perform each movement 3 times and rest in between. The movement was held during 3 seconds (contraction time) and the resting time was 3 seconds. To avoid inactivity periods being considered as movement related information due to delay between request and reaction, only 70 % of the contraction time was used. This percentage of the contraction time has been found to exclude inactive periods while keeping the dynamic portion of the contraction [16].
Sliding time windows of 200 ms with a 50 ms increment were used to extract a variety of signal features. The feature vectors were randomly distributed into sets for training (40%), validation (20%) and testing (40%) before training the classifiers. No data from the testing set was used during training and validation of the classifier.

C. Classification Complexity Estimating Algorithms

The CCEAs were designed to accept different numbers of channels and features, which allows for the estimation of classification complexity for individual and sets of features.

1) Separability Index: Separability Index (SI) for one class is defined as half the Mahalanobis distances (in features space) between the class and the center (mean of all dimensions) of its nearest class [12]. The distance in a two dimensional feature space is illustrated in Fig. 1 A.

The SI for a complete data set is computed by the average over all classes. See equation 1.

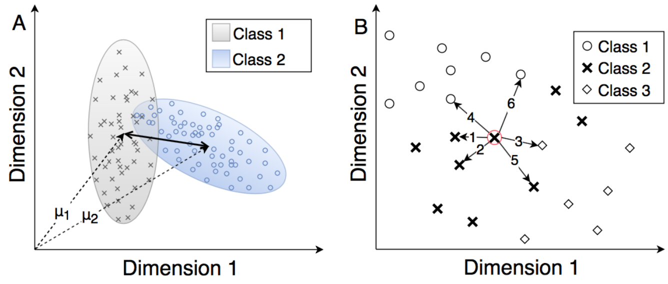

Fig. 1. Inset A shows the distance between the center points (mean of both dimensions) of two classes in a two dimensional feature space. The ellipses are constructed to represent the covariance of the classes. When the Separability Index is extracted, the distance is weighted by the covariance of the classes being compared. The bigger the weighted distance, the more separable the classes [12]. Inset B shows the six Nearest Neighbors for the target point marked by the red circle. By evaluating the dominance of Nearest Neighbors from the same class as the target point, an estimation of class separability can be established using all points in a data set as targets. Higher dominance equals higher separability [13].

$$SI = \frac{1}{c}\sum_{i=1}^{c}\left(\underset{j=1,\dots,i-1,i+1,\dots,c}{min} \frac{1}{2} \times \times \sqrt{(\mu_i-\mu_j)^T S_i^{-1}(\mu_i-\mu_j)} \right) \tag{1}$$

Where c is the number of classes, μ_i and μ_j are vectors of mean values, one for every dimension, and S_i is the covariance matrix of for the class i.
However, the Mahalanobis distance does not take the variance of the nearest class into account [15]. In order to investigate if this was limiting the algorithm, a list of commonly used statistical similarity measures was implemented as distance definition for SI. Their names and equations for multivariate normal distributions are listed below, starting with the original:

- Mahalanobis distance [15]

$$D_M = \sqrt{(\mu_1-\mu_2)^T S_1^{-1}(\mu_1-\mu_2)} \tag{2}$$

- Bhattacharyyas distance [14]

$$D_B = \frac{1}{8}(\mu_1-\mu_2)^T S^{-1}(\mu_1-\mu_2) + + \frac{1}{2} ln\left(\frac{detS}{\sqrt{detS_1 detS_2}}\right) \tag{3}$$

- Kullback-Leibler Divergence [14]

$$D_{KL} = \frac{1}{2}\left(tr(S_1^{-1}S_2) + (\mu_1-\mu_2)^T S_1^{-1}(\mu_1-\mu_2) - - k + ln\left(\frac{detS_1}{detS_2}\right)\right) \tag{4}$$

- Mahalanobis distance modified to take both covariance matrices into account:

$$D_{MM} = \sqrt{(\mu_1-\mu_2)^T S^{-1}(\mu_1-\mu_2)} \tag{5}$$

By this definition SI is related to the overlap shown in Fig. 1 A. Note the similarities with equation 3. The first term is completely included while the second is left out. The second term compares the shapes of the distributions. This is relevant for similarity measures but not for separability. *E.g.* if $\mu_1 = \mu_2$, the second term could still give a high value but class separation would be impossible. This distance definition will be referred to as Modified Mahalanobis.

For all equations μ_1 and μ_2 are vectors of mean values, one for every dimension, and

$$S = \frac{S_1 + S_2}{2} \tag{6}$$

where S_1 and S_2 are covariance matrices. Subscript 1 and 2 labels the two classes being compared.

2) Nearest Neighbor Separability: Nearest Neighbor Separability (NNS) measures how well the class of a data set is represented among their nearest neighbors (NNs) in feature space [13]. Fig. 1 B show the six NNs of a target member in a two dimensional feature space. Proportions of NNs from the same class as the target were calculated. The contribution of each NN was weighted differently depending on its proximity to the target point by calculating the average of the aforementioned proportions for all numbers of NNs 1,2,...,k, where k is the number of NNs taken into account. Equation 7 shows this step for the target member in Fig. 1 B.

$$\left(\frac{1}{1} + \frac{2}{2} + \frac{2}{3} + \frac{2}{4} + \frac{3}{5} + \frac{3}{6}\right) \Big/ 6 = 0.71 \tag{7}$$

The final result was the average over all members. In the original algorithm this was repeated for a set of different resolutions [13]. In this study only the resolution 1 was used, *e.i.* feature space was not divided into hyper cuboids.

D. Features

The following features were used in this study. In time domain; mean absolute value (tmabs), standard deviation (tstd), variance (tvar), waveform length (twl), RMS (trms), zero-crossing (tzc), slope changes (diff) (tslpch), power (tpwr), difference abs. mean (tdam), max fractal length (tmfl), fractal dimension Higuchi (tfdh) fractal dimension (tfd), cardinality (tcard) and rough entropy (tren). In frequency domain; waveform length (fwl), mean (fmn) and median (fmd).

E. Classifiers

The classifiers used in this study were LDA, Multi-Layer Perceptron (MLP), Support Vector Machine (SVM)(quadratic), and Regulatory Feedback Networks (RFN). These classifiers were used as implemented in BioPatRec [16] (code available online [17]), where LDA and SVM were implemented using pre-defined functions in Matlab.

F. Evaluation and Comparison

The data set was used in two ways. First, CCEs using individual features were compared with the resulting accuracy using only that feature. This served not only to obtain a wide range of CCEs, but also to rate the features adequacy as classifier inputs. Both accuracy and CCE were calculated for all classes and all subjects. Results given by use of individual classes are referred as individual results. Rating classes individually provided a wide CCE range as well as information about the EMG acquisition, i.e low separability for one class means high influence of error in that class. Averages over all classes were included in the result and referred as average results. Sets of 2-4 features were selected by ranking the results given by SI (Modified Mahalanobis) and NNS (k = 20) for all possible feature combinations including the feature with the highest CCE from individual feature evaluations, further referred to as *best sets*. Ortiz-Catalan proposed sets of 2-4 features found to be highly performing by a genetic algorithm [7]. These sets containing two and three features, and the Hudgins set, which is four out of five features introduced by Hudgins in [18], were used as benchmarking *reference sets*:

- **Ref 2:** tstd, trms [7]
- **Ref 3:** tstd, fwl, fmd [7]
- **Ref 4:** tmabs, twl, tslpch, tzc [18]

The *best* and *reference sets* of equal number of features were compared using different classifiers. Statistical significance was calculated with Wilcoxon signed-rank test ($p <= 0.05$). Since there was no clear linearity in the dependencies between accuracies and any CCEA, correlations were calculated using Spearmans rho.

III. Results

A. Separability Index

Correlations between SI and LDA accuracy when using the different statistical similarity measures as distance definitions are presented in Table I. Because the Modified Mahalanobis had higher correlation, and a more cohesive distribution with less outliers (see Fig. 2), it was selected as the distance definition for SI in following experiments.

TABLE I
SEPARABILITY INDEX CORRELATION WITH ACCURACY

	Individual Results	Average Results
Bhattacharyyas	0.79	0.83
Kullback-Leibler	0.78	0.69
Mahalanobis	0.85	0.78
Mahalanobis Modified	0.85	0.93

Correlations, using Spearmans rho, between accuracy and SI when using individual features classified by LDA. The statistical similarity measures in column one are used as distance definitions. Under individual results, correlations were calculated using values for every class while average over classes were used under column three.

In Fig. 3 accuracies using different classifiers are plotted against SI. All data corresponds to individual features. SVM and RFN results are more scattered compared with LDA and MLP results. They also have a considerable number of individual results close to zero accuracy, which seem uncorrelated with SI. The average results however, show high correlation between SI and accuracy for all classifiers.

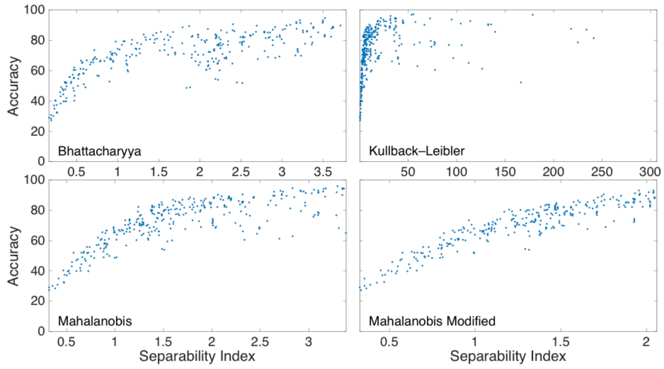

Fig. 2. Plots of accuracy against SI using individual features fed separately to LDA. The statistical similarity measure given in the plot is used as distance definitions. Accuracy and SI are average result over all classes.

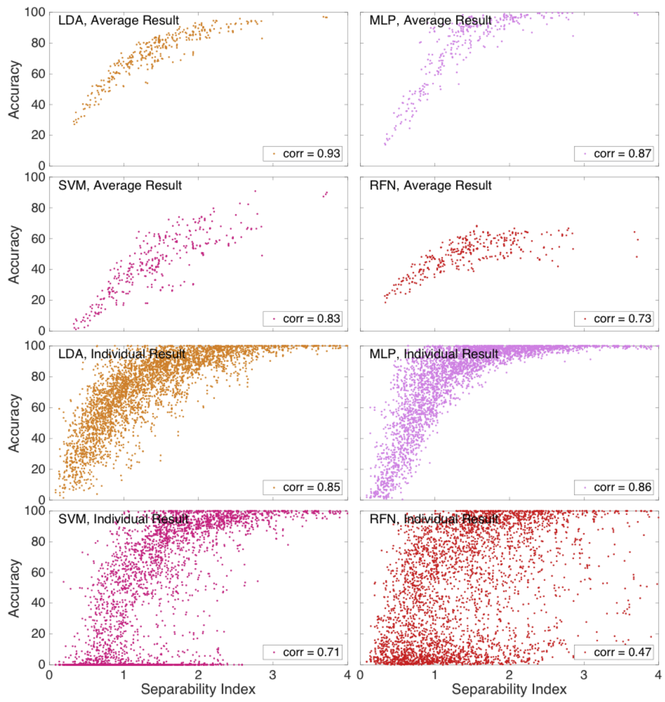

Fig. 3. Plots of accuracy against SI using individual features fed separately to the different classifiers. The top four show results that are average over all classes while the bottom four show result for classes individually. Correlation was calculated using Spearmans rho.

B. Nearest Neighbor Separability

The consequence of increasing the parameter k is that the algorithm becomes more sensitive to overlapping classes but it takes more iterations to compute. See how higher k increases correlation with accuracy along with the relative computation time in Table II. SI with Modified Mahalanobis uses 5.2 % of the computation time used by NNS with $k = 20$.

Plots of NNS results for different classifiers are shown in Fig. 4. Again individual results for SVM and RFN are

TABLE II
Nearest Neighbor Separability Correlation with Accuracy and Computation Time

	Individual Results	Average Results	Relative Time
k = 20	0.84	0.87	1
k = 40	0.86	0.88	1.37
k = 60	0.88	0.90	1.75
k = 80	0.89	0.91	2.14

Correlations, using Spearmans rho, between accuracy and NNS when using individual features fed separately to LDA and the values of k in the first column. Correlations under individual result are calculated using values for every class while average result is used for column three. Forth column shows the computation time relative to the fastest, k = 20.

widely scattered, but high correlation can still be found for all classifiers looking at the average result. However, NNS is spreading more for higher accuracies. This is especially clear in the average results for LDA where the plot is sun fan shape above 60 % accuracy and clustered around a line otherwise.

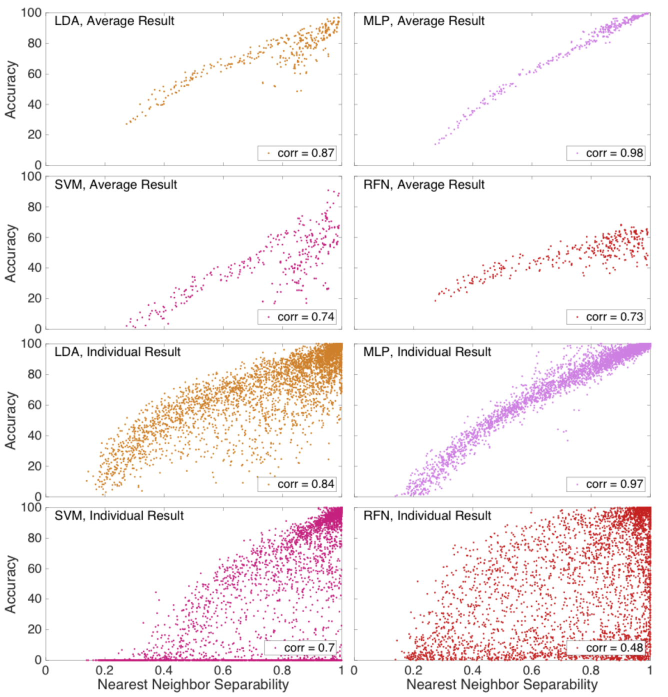

Fig. 4. Plots of accuracy against NNS using individual features fed separately to the different classifiers. The top four shows results that are average over all classes while the bottom four shows result for classes individually. Correlation was calculated using Spearmans rho.

C. Feature Sets

The classification accuracy from all classifiers when fed by the *best* and *reference sets* was used as evaluation method for performance. These results are illustrated in Fig. 5. Statistical significance is indicated by *. Correlation between CCEs and accuracies from using the *best* and *reference sets* are show in Fig. 6. Comparing Fig. 6 with Fig. 3 and 4 the results for LDA and MLP are similar except that accuracies are generally higher for feature sets over individual features. The SVM results are less scattered and neither RFN or SVM results are clustered at zero accuracy as in Fig. 3 and 4.

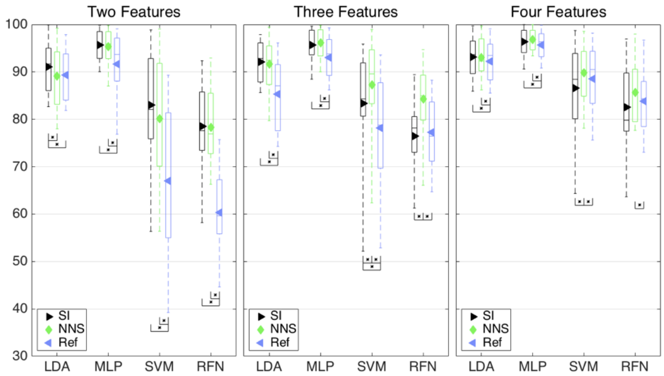

Fig. 5. Accuracies using the *best sets* from SI and NNS compared with the *reference sets*. The center line in the box is the median value, the marker is the mean value and the top and bottom are 25th and 75th percentiles respectively. The total data range is shown by the whiskers. Statistical significance using significance level 5 % is marked with *.

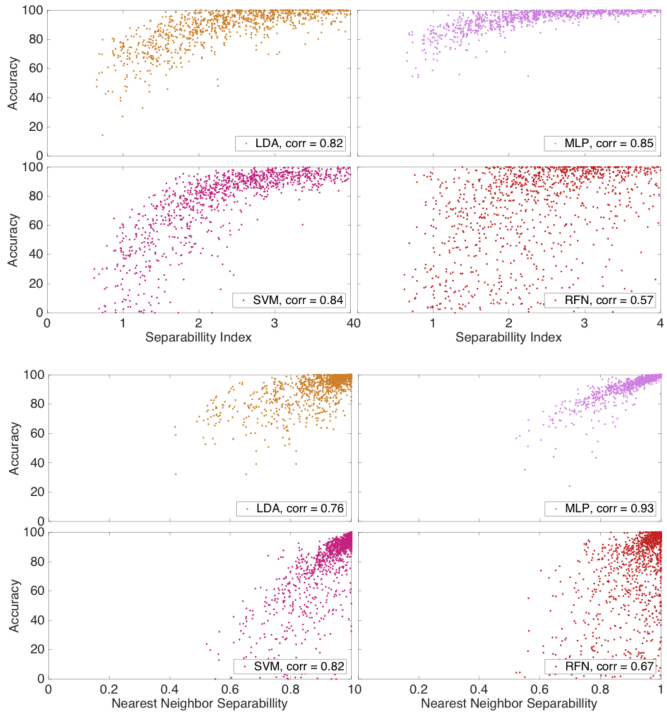

Fig. 6. Accuracy plotted against SI (top four insets) and against NNS (bottom four insets). The *best* and *reference sets* were used separately to extract feature vectors for all subject. One feature vector was fed to the classifier to create one point. Correlation was calculated using Spearmans rho.

D. Features

The rating of features and feature sets in this study has provided information on the features general performance. Fig. 7 shows the five features with highest and lowest average accuracy when using individual features. LDA and MLP results are represented. The five most selected features for the *best sets* are *tcard, fmn, tvar, tstd* and *tpwr* for SI and *tcard, tdam, tstd, twl* and *fmn* for NNS. The features are ranked in the order they are written, with the most selected feature first. It is worthy of notice that one of the top feature, cardinality, was recently found to be a highly performing feature in MPR [19].

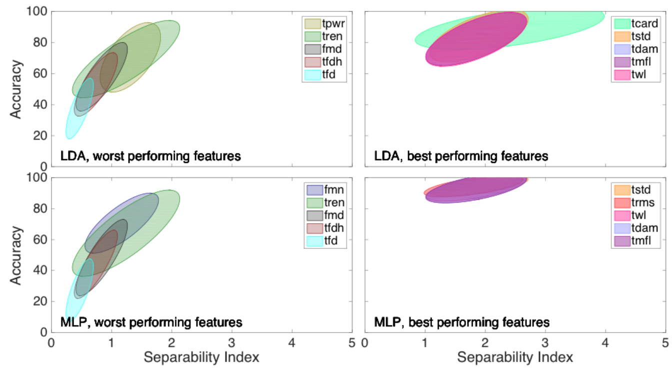

Fig. 7. Ellipses representing feature scatters of Accuracy against SI plots. The ellipses are drawn to represent the covariance matrix. The left insets show the features with the lowest average accuracy and the right insets show the features with the highest.

IV. Discussion

A. Accuracy Prediction

This study shows that NNS and SI can provide useful information when predicting accuracy for MLP and LDA based on the high correlation between classification accuracies and the CCEs, for both individual features and feature sets. This was also supported by the statistically significant improvement on MPR accuracy of the *best sets* over the *reference sets*. The only exception found was the *best set* of two features selected by NNS and fed to LDA which yielded lower accuracy than the *reference set*. However, the fact that these sets perform similarly is an indication that NNS provides relevant information for the problem at hand.

The SVM accuracy had low correlation with SI and NNS, compared to LDA and MLP, for individual features. However, correlation improved when feature sets were used, and the *best sets* are all yielded higher accuracy than the *reference sets*. How relevant the CCEs are for SVM seems to change with the number of inputs to the classifier.

All CCEAs evaluated in this study result in low correlation with RFN accuracy. However, all the *best sets* from NNS yielded significantly higher accuracy than the *reference sets*, which supports the use of this method for feature selection.

B. Consistency Over Change in Number of Dimensions

Consistency of SI and NNS for MLP and LDA can be appreciated by comparing the corresponding plots for individual features and feature sets. The clusters are forming similar patterns even though different number of dimensions were used. This is not true for SVM and RFN, where many of the individual results from individual features has accuracy close to zero. This makes these plots inconsistent with the corresponding patterns found for feature sets.

C. Limitations and Future Challenges

The CCEAs correlate differently with different classifiers accuracies. One reason is that neither SI or NNS describe the limitation of LDA due to its dependency on linearly separable classes. MLP is a nonlinear classifier and its accuracy is consequently more accurately estimated by the two CCEAs. Another reason is that SI assumes normality of the feature distributions while NNS does not. On the other hand, SI is much less computationally demanding. How PRAs and CCEAs are combined must be considered as CCEAs are implemented in more specific applications.

The data set for this study is limited to individual movements, four EMG channels and only offline accuracy was considered. To really evaluate how relevant the CCEAs are for MPR, further tests are needed with more diverse data sets.

This study shows that the information given by CCEAs can be used in feature selection for MPR. However, the feature sets in this study had maximum four features and there are only four recorded channels. The low number of dimensions makes brute-force search possible but the complexity will increase rapidly as the number of channels, features and/or classes increase. MFL and mRMR are two feature selection strategies already used for MPR, and are both examples of what is likely to be an important part of MPR in the future. The CCEAs in this study will have to be used strategically in a similar way to be efficient for feature selection.

Estimating accuracy without implementing a classifier allows early evaluation of recorded data. Classes with low separability can be recorded and evaluated again until desired separability can be confirmed. More research needs to be done on how to interpret CCEs when they are used for MPR.

V. Conclusions

Two Classification Complexity Estimating Algorithms, namely Separability Index and Nearest Neighbor Separability, were found adequate for MLP and LDA based on their high correlation with classification accuracy for both individual features and feature sets. High correlation with SVM accuracy was also observed for feature sets.

The two CCEAs were also found useful for EMG feature selection for all three aforementioned classifiers as feature sets selected based on level of separability given by the CCEAs resulted in higher or similar accuracies when compared with *reference sets*.

Acknowledgments

This study is supported by VINNOVA, Promobilia, and MedTech West.

References

[1] E. Scheme and K. Englehart, "Electromyogram pattern recognition for control of powered upper-limb prostheses: state of the art and challenges for clinical use," *Journal of rehabilitation research and development*, vol. 48, no. 6, pp. 643–660, 2011.

[2] M. Ortiz-Catalan, N. Sander, M. B. Kristoffersen, B. Håkansson, and R. Brånemark, "Treatment of phantom limb pain (PLP) based on augmented reality and gaming controlled by myoelectric pattern recognition: A case study of a chronic PLP patient," *Frontiers in Neuroscience*, vol. 8, no. 8 FEB, pp. 1–7, 2014.

[3] X. Zhang and P. Zhou, "High-Density Myoelectric Pattern Recognition Toward Improved Stroke Rehabilitation," *IEEE Transactions on Bio-Medical Engineering*, vol. 59, no. 6, pp. 1649–57, 2012. [Online]. Available: http://ieeexplore.ieee.org/xpls/abs_all.jsp?arnumber=6172561 http://www.ncbi.nlm.nih.gov/pubmed/22453603

[4] D. Tkach, H. Huang, and T. a. Kuiken, "Study of stability of time-domain features for electromyographic pattern recognition." *Journal of neuroengineering and rehabilitation*, vol. 7, p. 21, 2010.

[5] M. B. I. Reaz, M. S. Hussain, and F. Mohd-Yasin, "Techniques of EMG signal analysis: detection, processing, classification and applications," *Biological Procedures Online*, vol. 8, no. 1, pp. 11–35, 2006. [Online]. Available: http://www.springerlink.com/index/10.1251/bpo115

[6] N. Bu, O. Fukuda, and T. Tsuji, *A Recurrent Probabilistic Neural Network for EMG Pattern Recognition*. IGI Global, 2006, pp. 130–153.

[7] M. Ortiz-Catalan, R. Brånemark, and B. Håkansson, "Biologically inspired algorithms applied to prosthetic control," *The IASTED International Conference, Biomedical Engineering,*, no. BioMed, pp. 7–15, 2012.

[8] A. Phinyomark, P. Phukpattaranont, and C. Limsakul, "Feature reduction and selection for EMG signal classification," *Expert Systems with Applications*, vol. 39, no. 8, pp. 7420–7431, 2012. [Online]. Available: http://dx.doi.org/10.1016/j.eswa.2012.01.102

[9] J. Liu, X. Li, G. Li, and P. Zhou, "EMG feature assessment for myoelectric pattern recognition and channel selection: a study with incomplete spinal cord injury." *Medical engineering & physics*, vol. 36, no. 7, pp. 975–80, 2014. [Online]. Available: http://www.sciencedirect.com/science/article/pii/S1350453314000988

[10] H. C. Peng, F. H. Long, and C. Ding, "Feature selection based on mutual information: Criteria of max-dependency, max-relevance, and min-redundancy," *Ieee Transactions on Pattern Analysis and Machine Intelligence*, vol. 27, no. 8, pp. 1226–1238, 2005.

[11] C. Qiang, Z. Hongbo, and C. Jie, "The Fisher-Markov Selector: Fast Selecting Maximally Separable Feature Subset for Multiclass Classification with Applications to High-Dimensional Data," *Pattern Analysis and Machine Intelligence, IEEE Transactions on*, vol. 33, no. 6, pp. 1217–1233, 2011.

[12] N. E. Bunderson and T. a. Kuiken, "Quantification of feature space changes with experience during electromyogram pattern recognition control," *IEEE Transactions on Neural Systems and Rehabilitation Engineering*, vol. 20, no. 3, pp. 239–246, 2012.

[13] S. Singh, "Multiresolution Estimates of Classification Complexity," *IEEE Transactions on Pattern Analysis and Machine Intelligence*, vol. 25, no. 12, pp. 1534–1539, 2003.

[14] G. Nagy and X. Zhang, *Simple Statistics for Complex Feature Spaces*. London: Springer London, 2006, pp. 173–195.

[15] S. Raudys, *Measures of Data and Classifier Complexity and the Training Sample Size*. London: Springer London, 2006, pp. 60–68.

[16] M. Ortiz-Catalan, R. Brånemark, and B. Håkansson, "BioPatRec: A modular research platform for the control of artificial limbs based on pattern recognition algorithms." *Source code for biology and medicine*, vol. 8, no. 1, p. 11, 2013.

[17] M. Ortiz-Catalan, "Biopatrec," Januari 2016. [Online]. Available: https://github.com/biopatrec/biopatrec

[18] B. Hudgins, P. Parker, and R. Scott, "A new strategy for multifunction myoelectric control," *Biomedical Engineering, IEEE Transactions on*, vol. 40, no. 1, pp. 82–94, Jan 1993.

[19] M. Ortiz-Catalan, "Cardinality as a Highly Descriptive Feature in Myoelectric Pattern Recognition for Decoding Motor Volition," *Frontiers in Neuroscience*, vol. 9, no. 416, 2015. [Online]. Available: http://www.frontiersin.org/neural technology/10.3389/fnins.2015.00416/abstract